MARTIAN INVERSE PEDESTAL CRATERS – CHARACTERISTICS OF A NEW TYPE OF EJECTA MORPHOLOGY. S. Kukkonen and T. Öhman, Arctic Planetary Science Institute, Lihtaajantie 1 E 27, FI-44150 Äänekoski, Finland (soilekuk@gmail.com, teemu.ohman@planetaryscience.fi).

Introduction: In the eastern rim region of the Hellas basin, tens of small impact structures display a prominent “inverse pedestal” morphology (Fig. 1). The structures consist of a host crater – relatively fresh-looking and bowl-shaped simple crater, as small and recent impact craters typically are. However, instead of ejecta deposits the craters are surrounded by flat hollows, so called inverse pedestals (Fig. 2). As the extent and the planimetric shape of the hollows correlate with those of typical impact ejecta, we present that the hollows are ejecta deposits with an inverted relief.

This work introduces Martian inverse pedestal craters (IPCs) and their main characteristics. All the morphologic analyses and spatial measurements are based on full resolution images of the ConTeXt camera (CTX; ~6 m/px) [1] aboard Mars Reconnaissance orbiter (MRO) and the High Resolution Stereo Camera (HRSC; ~12.5 m/px) [2] aboard the Mars Express orbiter (MEX). Additional topographic investigations are based on both gridded and individual profiles of Mars Orbiter Laser Altimeter (MOLA; grid-spacing ~464 m) and HRSC-DTM (grid-spacing down to 100 m) [2−4]. The thermal inertia of the region has been investigated based on the night infrared datasets of Thermal Emission Imaging System (THEMIS; ~100 m/px) [5] aboard Mars Odyssey.

Analyses: All the IPCs are small; crater diameters vary from ~0.19 km to ~1.34 km (median 0.45 km) whereas the diameters of the hollows vary from ~0.6 km to ~5.9 km (median 1.2 km). Thus, the crater/hollow diameter relationship is ~0.2 to 0.5. Hollow planforms are mostly symmetrical and nearly circular, although zigzag margins can also be found. The sinuosity (lobateness) of the hollows [6] varies from 1.02 to 1.79 (median 1.08, mean 1.11). This is similar to typical ordinary pedestal crater sinuosities in the Martian mid- to high latitudes [7]. In HRSC DTM and MOLA data, the crater bowls and surrounding hollows cannot be distinguished from each other, because of the small size of the structures. Shadow measurements imply mainly depths of tens of meters for the hollows, up to ~100 m. In THEMIS IR night images, both the craters and the surrounding hollows are seen darker than most of the craters of the same size.

As some of the IPCs are located in the vicinity of fluvial and volcanic features (e.g., channels), it is possible that the hollows (i.e., inverse pedestals) were formed by ice sublimation or erosion by fluvial or volcanic processes, and the impact craters are then just conveniently superposed onto the depressions. However, the hollow/crater diameter ratio varies from 1.9 to 4.9 (median 2.9), which is a typical diameter relationship for proximal ejecta/crater systems (e.g., [8]). Thus, we present that the hollows are crater ejecta deposits modified to form an inverted relief because of the removal of material beneath.

The IPCs are located in an SW-trending depression, the Hesperia–Hellas trough, which connects the elevated Hesperia Planum with the Hellas basin and is partly filled by layers of volcanic and sedimentary materials [9]. About 60% of the IPCs cut the Tyrrhenus Mons flank material, consisting of pyroclastic and lava deposits [10−11] and deposited during the Late Hesperian to Early Amazonian [12−13]. About one-third of the structures are located in a Noachian/Hesperian unit of sedimentary, and probably volcanic and eolian material dissected by fluvial and volcanic erosion [10]. The remaining six craters cut smooth Hesperian plains, probably mix of sedimentary material and low-viscosity lava flows erupted from local fissures [10, 14−15]. We have not found IPCs in other parts of Mars, nor are we aware of their presence on other planetary bodies.

Discussion: The small size of the newly discovered IPCs implies that the formation mechanism of the inverted ejecta blankets is related only to the uppermost ~30–200 m of the surface, based on estimations of the excavation depths (e.g., [16−18]). Depressed and degraded ejecta deposits are evidence of removal of material. Because the craters are located in the Martian mid-latitude zone displaying several indications of past and probably contemporary ground ice (e.g., [19−21]), ice may play a significant role in the formation of the IPCs.

We present that the IPCs form as a result of a small impact into a fine-grained (pyroclastic?) material covered by an ice-rich mantle deposited during high obliquity periods. The ejecta blanket consists of a mix of ice and fine-grained debris (dark in THEMIS IR night images), and because of its lower albedo, it absorbs more energy than the surrounding light ice-rich layer. When the heat is transmitted to the ice matrix, the ejecta start to sink by melting into the ice, forming a depression [22−23]. The model explains why only craters with a diameter of ~0.19 km to ~1.34 km have this appearance; larger craters have a too thick ejecta deposit for transmitting heat to the ice-layer. Instead, smaller impactors do not penetrate through the ice-rich layer, because of which the formed ejecta do not contain enough rocky debris to substantially increase the absorption and, hence, the transmission of heat to the substrate. The fresh appearance of the craters implies that the IPCs have formed relatively recently, but not earlier than the Middle/Late Amazonian based on the stratigraphic analyses. Corresponding structures might have also formed earlier in the Martian history – however, they probably degraded afterwards because of the surface erosion and ice sublimation caused by obliquity changes.

Conclusion: Tens of small impact structures in the eastern Hellas rim region display prominent inverse pedestal morphology. To our knowledge, such an ejecta morphology has not been discussed before. The unique appearance is probably a result of a small impact into fine-grained material covered by an ice-rich layer. The fresh appearance of the craters implies that the inverse pedestal structures have formed relatively recently, during the Middle/Late Amazonian. The presence of pedestal impact craters on the eastern Hellas rim region implies that the region hosts an ice-rich layer the thickness of which varies from ~30 m to ~100 m.

References: [1] McEwen A. et al. (2007) *JGR Planets, 112*, E05S02. [2] Neukum G. et al. (2004) *Eur. Space Agency Spec. Publ. 1240*, 17-35. [3] Zuber M.T. et al. (1992) *JGR Planets, 97(E5)*, 7781–7797. [4] Gwinner K. et al. (2010) *EPSL, 294*, 506–519. [5] Christensen P.R. et al. (2004) *Space Science Reviews, 110*, 85-130 [6] Barlow N.G. (1994) *JGR., 99*, 10927-10935. [7] Kadish S.J. et al. (2009) *JGR, 114*, E10001. [8] French B.M. (1998) *Ch. 5*. In: *Traces of Catastrophe*, Houston: LPI p. 74–78. [9] Kostama V.-P. et al. (2009) *EPSL, 294,* 321-221. [10] Leonard G.J. and Tanaka K.L. (2001) *USGS,* Map I-2694. [11] Greeley R. and Crown D.A. (1990) *JGR, 95*, 7133-7149. [12] Crown D.A. et al. (1992*) Icarus, 100*, 1-25. [13] Gregg T. et al. (1998) *USGS Misc. Invest. Ser.,* Map I-2556. [14] Price K. (1998) *USGS Misc. Invest. Ser.*, Map I-2557. [15] Crown D.A. and Greeley R. (2007*) USGS Misc. Invest. Ser.*, Map I-2936. [16] Croft S.K. (1980) *LPS XI*, 2347-2378. [17] Croft S.K. (1985) *JGR, 90*, C828-C842. [18] Osinski G.R. et al. (2013) *Icarus 224*, 347-363. [19] Mustard J.F. et al. (2001) *Nature 412(6845),* 411-414. [20] Baker D. et al. (2010) *Icarus, 207,* 186-209. [21] Dundas C. et al. (2018) *Science*, *359*, 199-201. [22] Patterson E.A. (1984) *Journal of Glaciology, 30(106)*, 296-301. [23] Knight P.G. (1999) *Glaciers*, Cheltenham, Stanley Thornes, 161 pp.

Acknowledgements: The authors thank Kiwa Inspecta for supporting the study.

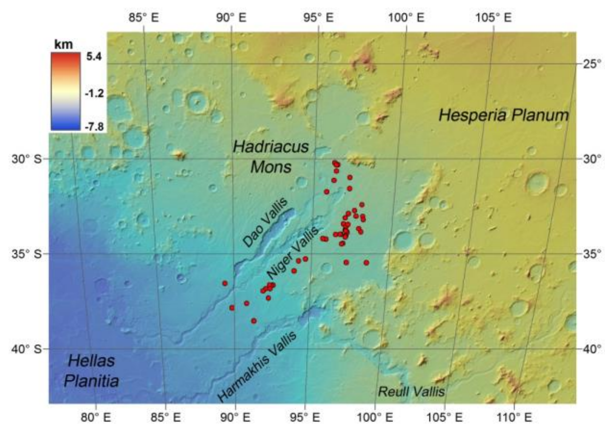

Figure 1. MOLA shaded relief of the eastern Hellas rim region. Red dots indicate the distribution of the inverse pedestal craters studied in this work.

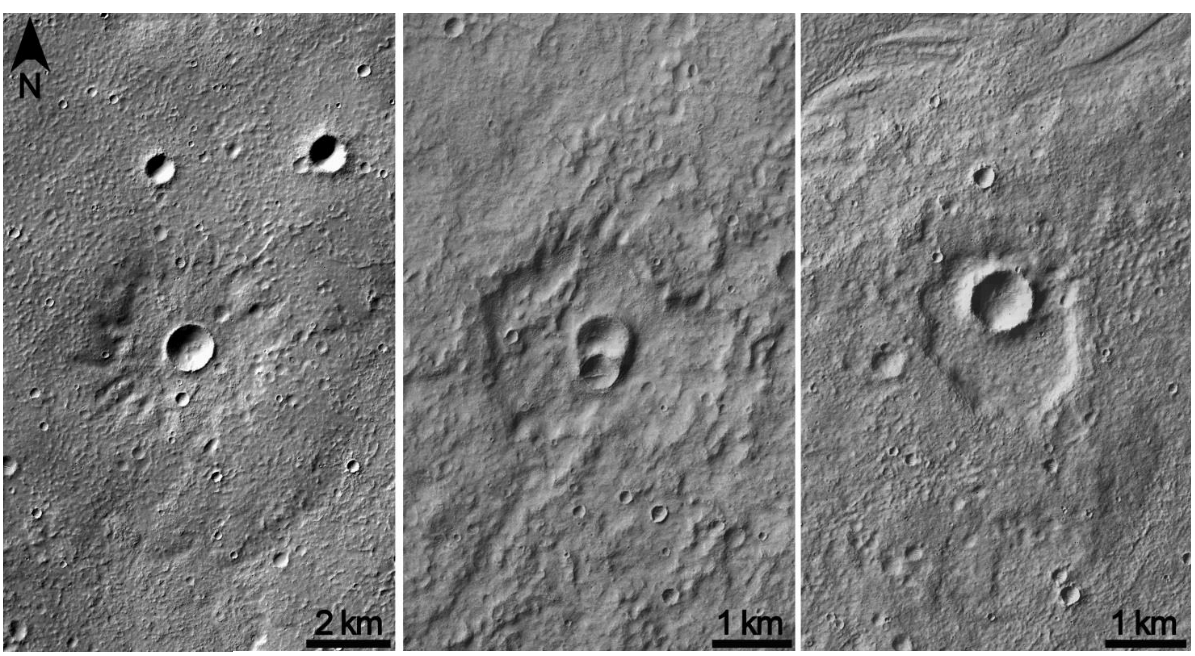

Figure 2. CTX images (P21_009111_1485_XN_31S263W, B17_016192_1463_XN_33S261W, and J02_045743 _1483_XN_31S262W) of inverse pedestal craters found in the eastern rim region of the Hellas basin.